Mathematical Biology and Bioinformatics
2022. V. 17. № S. P. t14–t29. doi: 10.17537/2022.17.t14

Ttranslation of the original article
Medvedev A.E., Golysheva P.S. Mathematical Biology and Bioinformatics. 2021;16(2):422–438.
doi: 10.17537/2021.16.422

========== TRANSLATIONS OF PUBLISHED ARTICLES ==========

Simulation of Air Motion in Human Lungs during Breathing. Dynamics of Liquid Droplet Precipitation in the Case of Medicine Drug Aerosols

Medvedev A.E., Golysheva P.S.

Khristianovich Institute of Theoretical and Applied Mechanics, Siberian Branch, Russian Academy of Sciences, Novosibirsk, Russia

Abstract. The paper deals with numerical simulation of the air flow in the full human bronchial tree. In their previous studies, the authors developed an analytical model of the full human bronchial tree and a method of stage-by-stage computation of the respiratory tract. A possibility of using the proposed method for a wide range of problems of numerical simulations of the air flow in human lungs is analyzed. The following situations are considered: 1) steady inspiration (with different flow rates of air) for circular and "starry" cross sections of bronchi ("starry" cross sections models some lung pathology); 2) steady expiration; 3) unsteady inspiration; 4) precipitation of medical drug aerosol droplets in human bronchi. The results predicted by the proposed method are compared with results of other researchers and found to be in good agreement. In contrast to previous investigations, the air flow in the full (down to alveoli) bronchial tree is studied for the first time. It is shown that expiration requires a greater pressure difference (approximately by 30 %) than inspiration. Numerical simulations of precipitation of medical drug aerosol droplets in the human respiratory tract show that aerosol droplets generated by a standard nebulizer do not reach the alveoli (the droplets settle down in the lower regions of the bronchi).

Key words: *bronchial tree, numerical simulation, human lungs, aerosol drugs, respiratory tract.*

INTRODUCTION

Breathing is a necessary vital function of the human organism, which is affected (sometimes adversely) by external factors. Air pollution is one of the basic problems nowadays. It was shown [1] that fine particles (smaller than 0.1 μm) of aerosols contained in city air reduce respiratory system functioning of adults and children with a higher probability than rough particles (greater than 0.5 μm). On the other hand, the inhaling (aerosol) method of drug delivery is widely used in medicine. This method offers a number of significant advantages over other methods of drug delivery because it acts directly at the pathology location. There are many old lung diseases, and there appear new ones. Successful treatment of such diseases, in addition to appropriate drugs, require knowledge of specific features of the air flow in the complex structure of human lungs.

The human respiratory system consists of the upper (nose, nasal pharynx, and larynx) and lower (trachea, bronchial tree, and alveoli) respiratory tracts. Human bronchi have a

complicated tree-shaped structure consisting of millions of bronchi ending with alveoli. The characteristic size of the bronchi decreases by a factor of 240 as the bronchial tree "grows." Therefore, construction of the full human bronchial tree and calculation of the air flow in human lungs is an extremely complicated and labor-consuming problem.

To construct the bronchial tree, Weibel [2] in 1963 described the anatomical model of the lower respiratory tracts, based on morphometry of human lungs. He proposed a model of symmetric dichotomy of the bronchial tract consisting of 24 bifurcations (points of division) of bronchi up to alveolar sacs and indicated the bronchus parameters (length and diameter, while the angle of bronchus bifurcation was not specified).

There are also other models of bronchial tree design. Nowak et al. [3] made an attempt to solve this problem by using series of consecutively reduced models of respiratory tracts. The input boundary condition applied at each respiratory tract segment was the result obtained by modeling the previous segment. One of the problems encountered in this type of consecutive procedures was the necessity of imposing the output boundary condition at the end of each segment prior to computations. A similar method was used in [4] to develop a model based on that proposed in [2]. Though both investigations ensured significant progress in modeling the air flow in human lungs, this consecutive procedure did not allow full flow connection at all levels.

Methods of constructing the bronchial tree based on computer tomography images (CT-Scan) of human lungs have been developed in recent years. A review of realistic anatomical models can be found in [5]. Various methods of visualization and processing of results for constructing 3D models of respiratory tracts were used to develop models of human lungs. Most of the models of the human bronchial tree contain less than ten bifurcations of bronchi [5]. A comprehensive review of the methods used to construct the human bronchial tree can be found in [9, 10]. The maximum number of bronchial tree bifurcations was 15 [6], 16 [11–13] (one branch of the tree was constructed), and 17 [7, 8].

Numerical computations of the air flow in the full human bronchial tree were impossible because the constructed tree was incomplete. The computations were performed only up to the 15-th ([6]), 16-th ([11–13]), and 17-th ([7, 8]) bifurcation. The computations were carried out over the entire domain of the bronchial tract (the computational domain included all constructed bronchi of the tree, which had many branches despite being incomplete). Therefore, the computations of the air flow required large computational resources. The reasons were different scales in the computational domain (the sizes of the upper and lower bronchi differ approximately by a factor of 240) and a large number of bronchus branches. The number of bronchi in the bronchial tree computations increased in a geometric progression. In [11–13], the computational domain was reduced to one branch of the tree (up to the 16-th bifurcation), but it was necessary to perform many iterations (up to one thousand of repeated computations) to match the flow in truncated branches. The air flow in human lungs was computed up to now only until the 17-th bifurcation [7, 8] out of 23.

The analytical model of constructing the full human bronchial tree for symmetric and asymmetric dichotomy was described in our previous papers [9, 10]. The computations of the air flow and drug aerosol precipitation in human bronchi discussed below were performed on the basis of the full human bronchial tree model with symmetric dichotomy [9]. A brief description of the stage-by-stage computation can be found in [14]. The goal of the present study is to demonstrate the possibility of using the authors' algorithm of bronchial tree design and the method of stage-by-stage computation in the full (up to alveoli) human respiratory tract for modeling a large class of problems of the air flow and precipitation of drug aerosols or particles in human lungs.

Mathematical Biology and Bioinformatics. 2022. V. 17. № S. doi: 10.17537/2022.17.t14

1. METHOD OF STAGE-BY-STAGE COMPUTATION OF THE FULL HUMAN BRONCHIAL TREE

Parameters of the human bronchial tree based on symmetric dichotomy

The human bronchial tree consists of bronchi connected by bifurcations (branching into two output bronchi) and has a complicated tree-shaped structure. To describe the human bronchial tree, Weibel [2] proposed a model of symmetric dichotomy, where the bronchi of one generation (number of the bronchus bifurcation) have identical parameters. There are 24 such bifurcations: the bronchial tree bifurcation parameter n changes from 0 to 23. The parameters of the model with symmetric dichotomy are described by the following expressions [11]:

- input bronchus parameter (in mm)

$$R_n = \begin{cases} 9e^{-0.388n}, & n \le 3 \\ 6.5e^{-(0.2929-0.00624n)n}, & n > 3 \end{cases}; \tag{1}$$

- input bronchus length (in mm)

$$L_n = \begin{cases} 120e^{-0.92n}, & n \le 3 \\ 25e^{-0.17n}, & n > 3 \end{cases}. \tag{2}$$

Functions (1) and (2), which describe the bronchus parameters, are plotted in Figure 1.

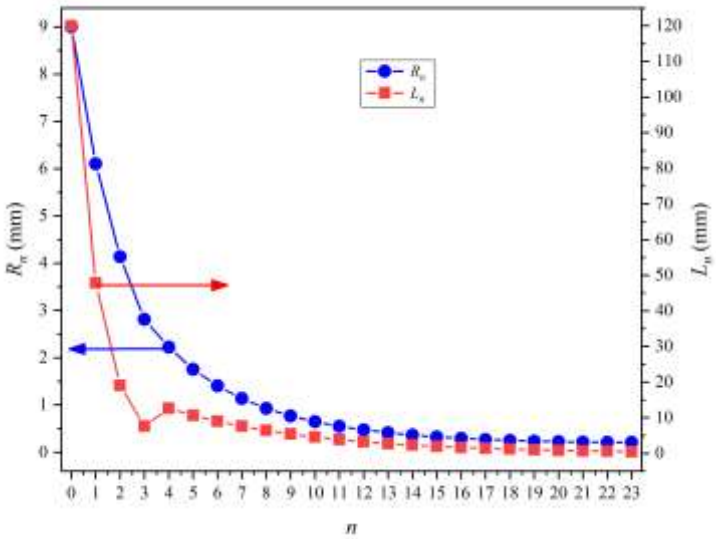

Fig. 1. Bronchus radius R_n (1) and length L_n (2) in a symmetric human bronchial tree.

Analytical design of the bronchial tree

For numerical simulation of bronchi, it is necessary to design a 3D model of the computational domain. Incorrect design of the problem geometry affects the accuracy of computations. A review of various methods of human bronchial tree construction can be found in [9, 10].

In our previous publications, we constructed an analytical model of the full bronchial tree with symmetric [9] and asymmetric [10] dichotomy (branching) of bronchi. The model [9] ensures easy design of bronchi with a circular or “starry” cross section. An example of the bronchial tree designed in accordance with the analytical formulas [9] is shown in Figure 2. The “starry” cross section of the bronchi simulates pathological constriction of bronchi.

Figure 2,a shows the bronchial tree up to the 5-th generation inclusive with a “starry” cross section of bronchi (bifurcations of the same generation are marked with the same color). It is impossible to show the full bronchial tree up to the 23-rd generation because there are too many bronchi. Figure 2,b shows one branch of the bronchial tree (only bifurcations adjacent to the right-side output bronchi) up to the 23-rd generation inclusive. By using the algorithm proposed in [9], it is possible to construct an arbitrary full branch of the respiratory tract with both circular and “starry” cross sections. The number and length of the “star” rays are defined parametrically and vary within wide limits.

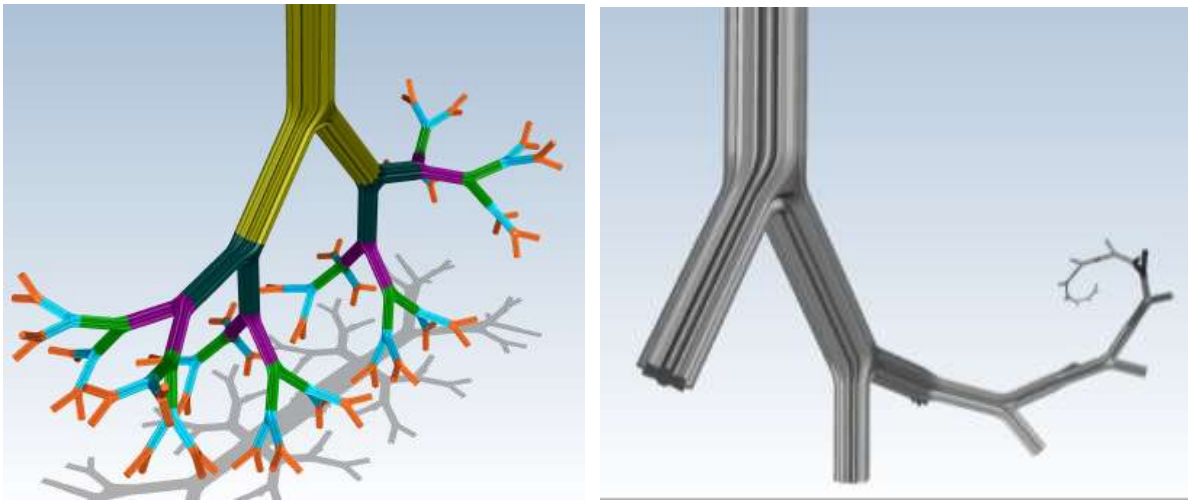

a) **b**)

Fig. 2. Examples of the human bronchial tree with “starry” bronchi designed on the basis of the proposed model [9]. (**a**) Bronchial tree up to the 5-th generation (branches of the same generation are marked by the same color). (**b**) One branch of the bronchial tree from the 0-th to 23-rd generation of bronchi.

Characteristics of air for modeling the flow in the bronchial tree

The air flow in the human bronchial tree was computed based on the model of a viscous incompressible fluid owing to low compressibility of air at pressures typical for the human respiratory tract. The same simplification of the problem was applied earlier in [11–13].

The air parameters used in the computations are the density $\rho = 1.23$ kg/m^3 and dynamic viscosity $\mu = 1.79 \cdot 10^{-5}$ Pa·s. These parameters of air are used in all computations discussed below. The flow rate of inhaled air for an adult at rest is $Q = 5$ l/min and increases to 140 l/min in the case of middle-distance racing. The maximum pressure drop in human lungs is $\Delta p \approx 35$ mm $H_2O \approx 343$ Pa [15, 16]. Thus, the maximum pressure difference in human lungs is of atmospheric pressure.

According to the bronchial tree design (symmetric dichotomy), the integral flow parameters, such as the flow rate and mean velocity, are identical for branches of the same generation. The mean flow velocity U_n and the Reynolds number Re_n at the output of the n-th bifurcation are calculated by the formulas

$$U_n = \frac{Q}{2^n \pi R_n^2}, \qquad \mathrm{Re}_n = \frac{2\rho U_n R_n}{\mu} = \frac{\rho Q}{2^{n-1} \pi \mu R_n}. \tag{3}$$

The air flow rate in each bronchus and the mean flow velocity are known in advance, before the numerical solution of the problem, which yields the pressure in the bronchi and the flow velocity distributions over the bronchus cross sections.

The mean velocity and Reynolds number calculated by Equations (3) are shown in Figure 3. The critical Reynolds number for a circular tube with smooth walls is 2300. It is

seen from Figure 3 that the Reynolds numbers are higher than the critical value only for several large bronchi at the flow rate of 50 l/min, while the flow at the flow rate of 25 l/min is laminar in all bronchi. For people at rest, at flow rates smaller than 25 l/min, the flow in the entire human bronchial tree is laminar in accordance with the criterion of the critical Reynolds number.

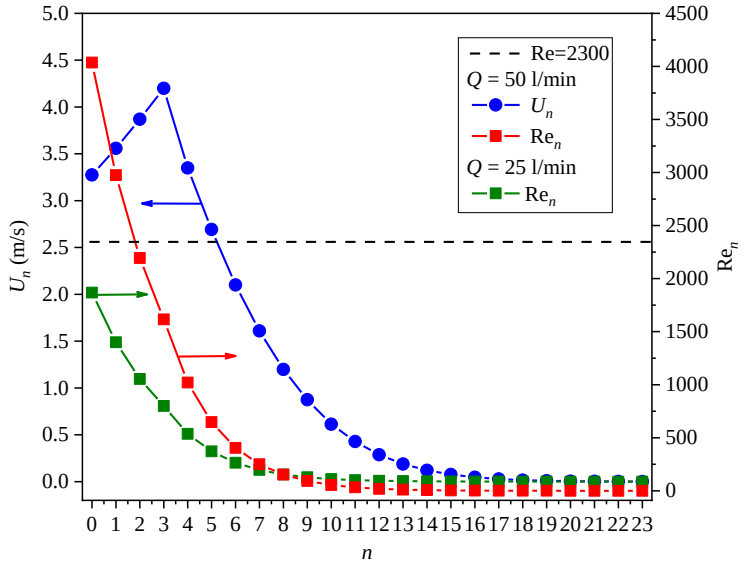

Fig. 3. Mean velocity U_n and Reynolds number Re_n of the flow at the output of the n-th bifurcation (formula (3)) for the air flow rates of 25 and 50 l/min.

For bronchi with a "starry" cross section, the Reynolds number is calculated on the basis of the hydraulic radius (radius of a tube with an equivalent surface) and is slightly higher than that for a circular tube.

Method of calculating the flow in the bronchial tree

The simulations were performed within the framework of the Navier-Stokes equations for a viscous incompressible fluid

$$\nabla \cdot \vec{v} = 0,$$
$$\rho\left[\frac{\partial \vec{v}}{\partial t} + (\vec{v} \cdot \nabla)\vec{v}\right] = -\nabla p + \mu \nabla^2 \vec{v}, \tag{4}$$

where $\vec{v}$ is the air velocity, p is the air pressure, μ is the dynamic viscosity coefficient, and ρ is the air density.

The bronchi are numbered from 0 (trachea) to 23 (terminal bronchioles, which are the last bronchioles before the alveoli). The bronchus radius R_n and length L_n are determined by formulas (1) and (2).

The method of bronchial tree computation was considered in [16]. The numerical technique of stage-by-stage computation of the human bronchial tree includes the following stages:

1) An arbitrary branch of the bronchial tree is chosen (of an arbitrary shape, with a sequence from the 0-th to 1-st bifurcation, then to the 2-nd bifurcation, etc., up to the 23-rd bifurcation);
2) The bronchus geometry from the 0-th to 23-rd bifurcation is analytically designed;
3) The input value of the flow rate of inhaled air Q at the trachea at $n = 0$ is prescribed;

4) The air flow rate at the output of the n-th bifurcation is determined by the formula $Q_n = Q/2^{n+1}$ $(n = 0,1,..,23)$;

5) At the input of the 0-th bronchus, the pressure $\tilde{p}_0$ averaged over the cross section and the gas velocity distribution $\vec{u}_0(x,y,z)$ are specified (the pressure and velocity distribution are found by solving the problem of the air flow in the nasal farynx; for simplicity, it is possible to use the atmospheric pressure and velocity distribution from the Poiseuille solution); the gas flow rate at the output of the 0-th bifurcation is set as $Q_0 = Q/2$;

6) The air flow in the 0-th bifurcation is numerically calculated; after solving the problem, we find the gas velocity distribution at the output $\vec{u}_1(x,y,z)$ and the pressure averaged over the cross section $\tilde{p}_1$;

7) For calculating the flow in the n-th bifurcation, the input data are the velocity distribution at the output of the previous bifurcation $\vec{u}_{n-1}(x,y,z)$ and the mean pressure $\tilde{p}_{n-1}$; the air flow rate $Q_n = Q/2^{n+1}$ $(n = 1,...,23)$ is specified at the output; after solving the problem, we find the gas velocity distribution at the output $\vec{u}_n(x,y,z)$ and the mean pressure $\tilde{p}_n$;

8) Stage 7 is repeated for all bifurcations up to the 23-rd bifurcation.

Remark:

1) the mean velocity of the gas at the output of the n-th bifurcation $\tilde{u}_n$ can be easily determined from the gas flow rate at the output Q_n; as the flow rate at the output is imposed as the boundary condition, the computed velocity accurately coincides with the theoretical prediction;

2) the computed pressure $\tilde{p}_n$ is independent of the chosen branch of the bronchial tree because the pressure in all bronchi of the n-th bifurcation is identical (according to the model [9], the bronchi of the next bifurcation are turned along the axis of the bronchus branch by the angle $\pi/2$, thus, providing local symmetry for the generation of bifurcation being considered);

3) the gas flow in an individual bronchus is comparatively simple and can be computed by almost all CFD codes;

4) the time of stage-by-stage computation is the sum of the time needed to compute one bifurcation multiplied by 24 (total number of bifurcations);

5) the time needed to compute one bifurcation varies from several minutes to several tens of minutes (depending on the desired accuracy of simulations).

The stage-by-stage computation of the bronchial tree is schematically illustrated in Figure 4,a. Figure 4,b shows the result of matching the velocity fields in the transition from the 0-th to 1-st bifurcation.

The proposed method differs from the previously available methods. Tena et al. [11] calculated one bronchial branch up to the 16-th bifurcation without side branching. Flow matching in truncated branches was ensured by the method of successive approximations (thousands of iterations). However, the computations [11] were performed for a turbulent flow, and the pressure difference was overestimated. The computation of the entire branch of the bronchial tree and the method of successive approximations required a large computational time (up to five days [11]).

Mathematical Biology and Bioinformatics. 2022. V. 17. № S. doi: 10.17537/2022.17.t14

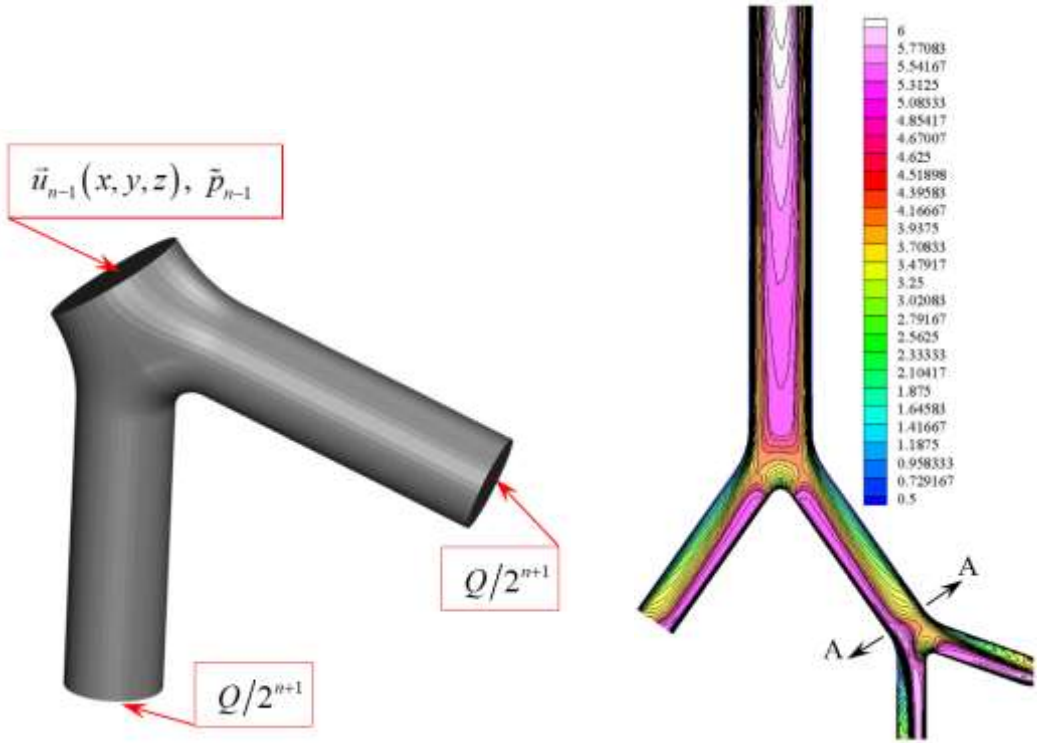

a) **b**)

Fig. 4. (**a**) Schematic of stage-by-stage computation of the human bronchial tree. (**b**) Computed isolines of the absolute value of velocity in the 0-th and 1-st bifurcations. The computations are performed for the air flow rate of 50 l/min. The flow velocity is given in m/s. The place of bifurcation matching is indicated by AA.

2. APPLICATION OF STAGE-BY-STAGE COMPUTATION FOR STUDYING THE AIR FLOW IN HUMAN LUNGS

Steady inspiration for bronchi with circular and "starry" cross sections

Steady inspiration for the tree with bronchi of circular and "starry" cross sections was numerically simulated. The following parameters were taken for "starry" bronchi: the normalized height of the "star" rays is $s_{\text{ob}} = 0.4$, the number of rays in the "star" is $n_{\text{ed}} = 8$, and the cross-sectional area of the obstructed bronchus coincides with the area of the circular bronchus (the formulas for design of "starry" bronchi can be found in [9]). The computations were performed for the branch shown in Figure 2,b (only the "starry" branch is shown here). As it was mentioned above, the results of calculating the pressure in the bronchial tree are independent of the branch choice: the pressure values are identical in all bronchi of one bifurcation number.

The results of simulating the bronchial tree up to the 23rd bifurcation inclusive are presented in Figure 5, which shows the difference in the mean (averaged over the cross-sectional area) pressure $\Delta p_n = p_0 - p_n$ between the input of the 0-th bronchus and the output of the n-th bronchus. For comparison, the data [11] (up to the 16-th bifurcation) obtained with the turbulent flow model are also plotted. It is seen that the turbulent flow model leads to overestimation of the pressure difference (curve (a) in Fig. 5) as compared to the laminar flow case (curve (b) in Fig. 5). The allowance for the real "starry" shape of the bronchi leads to significant enhancement of the pressure drop in the respiratory tract (curve (c) in Fig. 5). The proposed model allows modeling "starry" constriction of bronchi in the pathological case.

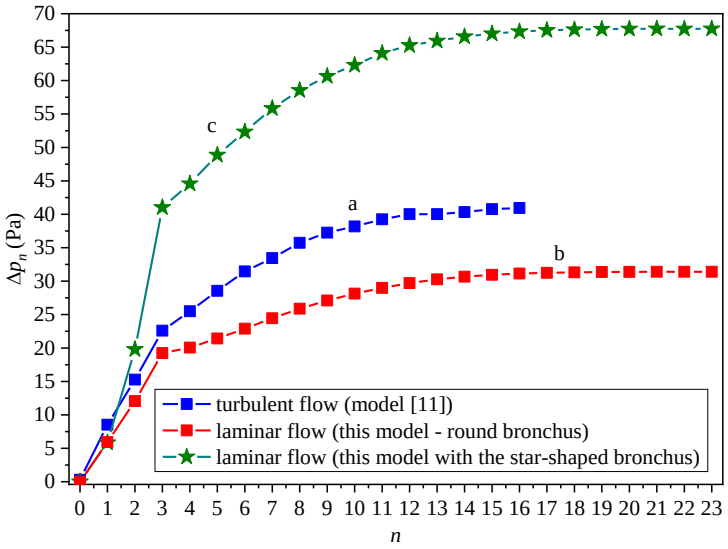

Fig. 5. Results of the numerical simulation of the air flow for the case of inspiration in the human bronchial tree for the flow rate of 50 l/min. The computations are performed for (**a**) the tree with circular bronchi [11]; (**b**) the tree with circular bronchi; (**c**) the tree with "starry" bronchi. The results (**b**) and (**c**) are obtained by using the proposed model.

A series of simulations was performed for the pressure difference in bronchi for different flow rates of air. It is seen that the pressure difference in the lungs increases with an increase in the flow rate of inhaled air (Fig. 6).

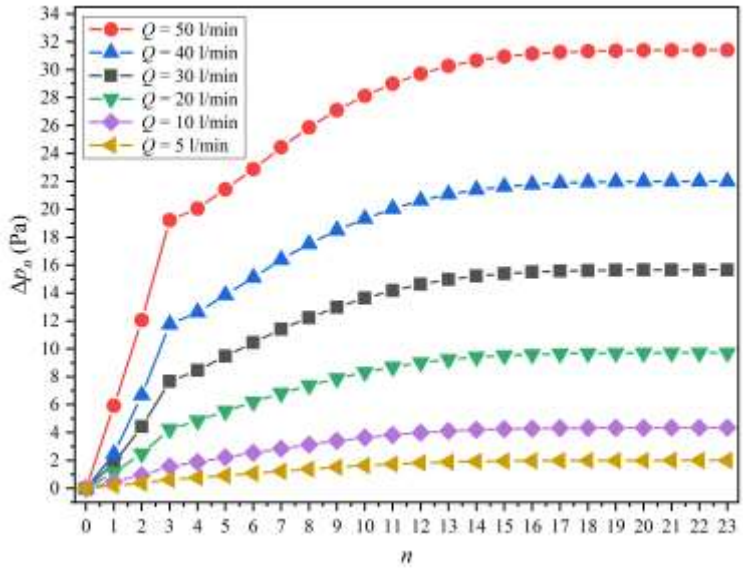

Fig. 6. Results of numerical simulations of the pressure drop in the human bronchial tree (with circular bronchi) for flow rates ranging from 5 to 50 l/min in the case of inspiration.

Using CT-Scan images, Islam et al. [7] designed a model of human lungs for a particular person. This model contains only the upper 17 generations of the human bronchial tree. Based on the resultant bronchial tree, Islam et al. [7] computed the pressure difference in the lungs for five different branches of the bronchial tree. In contrast to Figures 5 and 6, they plotted the pressure difference $\delta p_n = p_n - p_{23}$. The pressure differences computed in [7] and in the present study are compared in Figure 7. The difference in the pressure values in bifurcations with small numbers, similar to comparisons of Figures 5 and 6, can be explained by the fact that the computations [7] were performed with the turbulent model of the air flow, whereas our computations were carried out for the laminar case. The tree geometries were also different.

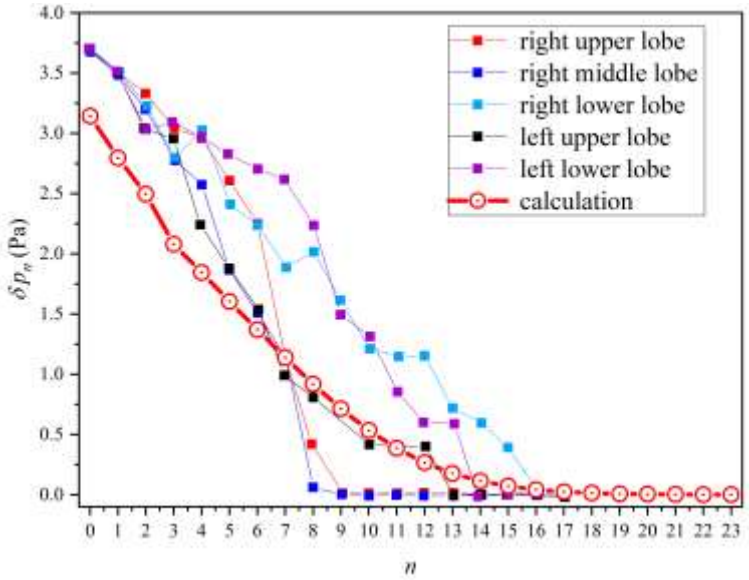

Fig. 7. Computed pressure difference along the bronchi in the case of inspiration with the flow rate of 7.5 l/min. The squares show the results computed in [7] for five different branches of the bronchial tree up to the 17-th generation of bronchi. The circles are the results predicted by the proposed model up to the 23-rd generation of the bronchial tree.

Steady expiration for bronchi with a circular cross section

The air pressure in the case of expiration was also calculated. The results are summarized in Figure 8. The computations show that the pressure difference in the case of expiration is greater (approximately by 30 %) than that in the case of inspiration. The reason is flow compression when passing from the lower to upper bronchi in the case of expiration. According to Equation (1), the total cross-sectional area of the bronchi of the 23-rd generation is greater than the trachea cross-sectional area by a factor of $\left(R_{23}/R_0\right)^2 \cdot 2^{23} \approx 4500$.

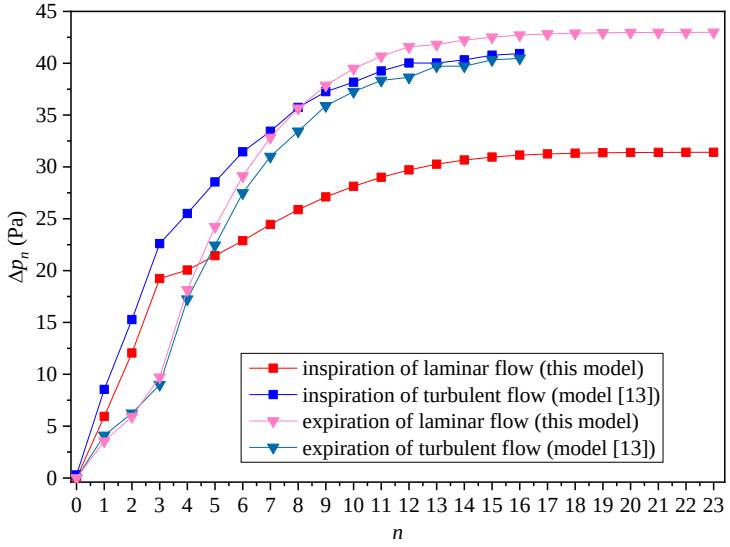

Fig. 8. Results of numerical simulations of inspiration and expiration for the flow rate of 50 l/min. Comparison of the results computed with the proposed model and with the model [13].

Tena et al. [13] performed computations for a turbulent gas flow (which is responsible for an almost twice higher pressure value) for an incomplete branch up to the 16-th bifurcation. However, there was probably a mistake in the computations of the expiration pressure [13]: the expiration resistance should be greater than the inspiration resistance. This was

demonstrated in our computations: the pressure difference of expiration is greater by a factor of 1.3 than the pressure difference of inspiration (Fig. 8).

Unsteady inspiration for bronchi with a circular cross section

A situation of unsteady inspiration was also calculated. The initial parameters of inspiration were taken to be the results of standard spirometry [17]. The plot of inhalation spirometry is shown in Figure 9. Numerical simulations were performed for unsteady inspiration only. The selected inspiration region is marked in Figure 9.

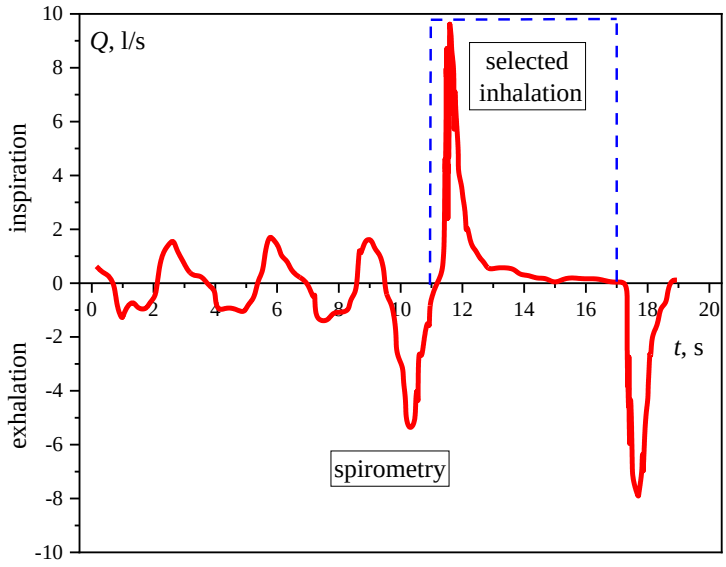

Fig. 9. Plot of standard spirometry [17] with a selected inspiration region.

The nasal pharynx was modeled with the use of a 3D model obtained on the basis of cross sections from [12]. The pharynx model is shown in Figure 10. As the main emphasis in the present study is made on the air flow in the bronchial tree, a simplified version of the pharynx was used in numerical simulations. Therefore, the details and specific features of the air flow in the pharynx are not considered here. The air flow in the pharynx and the influence of the nose shape on the air flow were studied in much detail in [18–21]. In our computations, we only considered air inhalation through the mouth.

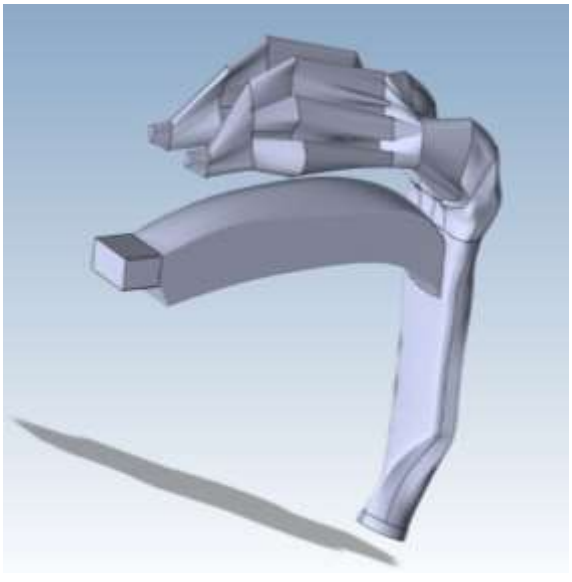

Fig. 10. Simplified computational model of the human pharynx.

As in [12], the original spirometry was simplified: the inspiration spirometry was divided into 20 regions with a constant flow rate, and the computations were performed in a quasi-steady regime. The validity of such a quasi-steady approach to calculating unsteady spirometry was justified in [12]. The spirometry was divided in the following way: ten regions of 1 liter per second for increasing and decreasing flow rates (see the selected inspiration region in Fig. 9). Such a division allowed us to include important changes in the initial flow and avoid non-relevant aspects of the problem.

The results of numerical simulations of unsteady inspiration are shown in Figure 11. It is seen that the pressure difference at the output of the 23-rd bifurcation increases (as compared to the input difference in pressure), but the shape of the pressure curve as a function of time remains the same.

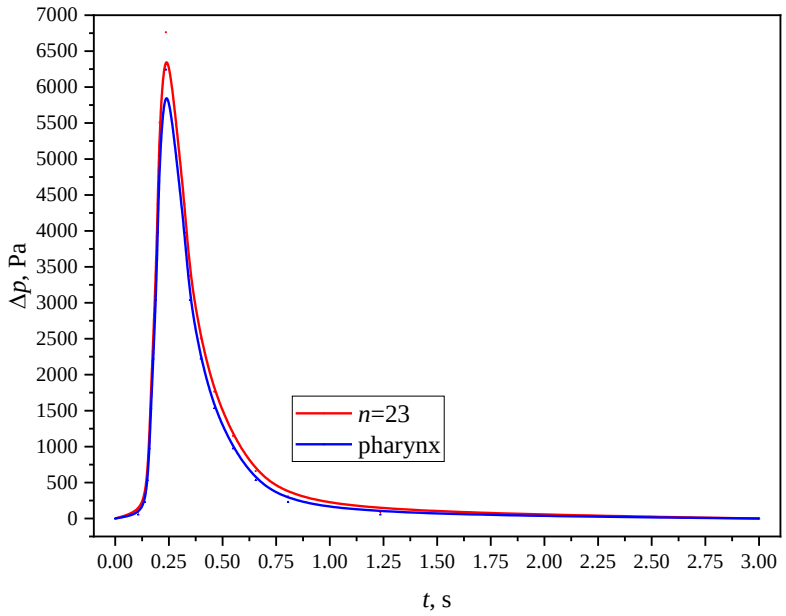

Fig. 11. Pressure difference at the pharynx output (blue curve) and at the output of the 23-rd bifurcation (red curve) for unsteady inspiration (selected region of spirometry in Fig. 9).

3. APPLICATION OF STAGE-BY-STAGE COMPUTATION FOR STUDYING AEROSOL PRECIPITATION IN BRONCHI

Precipitation of particles in the human respiratory tract was modeled by many researchers ([11, 15, 16] and others), but the computations did not reach the lower branches of bronchi, leaving aside alveoli, because of the limitations due to bronchial tree incompleteness. The proposed model allows the motion of droplets (or particles) to be tracked up to alveoli.

Precipitation of drug aerosol droplets in human lungs was computed. We used a typical compressor nebulizer NE-C24 produced by the Omron company. The nebulizer had the following parameters: droplet size 3 μm and volume flow rate of the aerosol 0.3 ml/min. The air flow rate for aerosol inhaling through the nebulizer was varied from 20 l/min (which corresponds to the normal volume of human lungs) to 50 l/min (which corresponds to a very large volume of human lungs). The inspiration duration was 1 s. After incidence onto the bronchus walls, the droplets stuck to them.

The equation of motion of aerosol droplets is

$$m_p \frac{d\vec{v}_p}{dt} = \vec{F}_D \tag{5}$$

where the force is $\vec{F}_D = \frac{m_p\left(\vec{v}-\vec{v}_p\right)}{\tau_p}$, $\vec{v}$ and $\vec{v}_p$ are the gas and droplet velocities, respectively, m_p is droplet mass, the characteristic time of velocity stabilization is determined by the Hadamard-Rybczynski equation [22] in the form $\tau_p = \frac{4\rho_p d_p^2}{3\mu C_D \mathrm{Re}_p}$, $C_D = \frac{8}{\mathrm{Re}_p}\left(\frac{2+3k}{1+k}\right)$, $k = \frac{\mu_p}{\mu}$, where μ and μ_p are the dynamic viscosity coefficients of the gas and droplets, respectively, and d_p is the droplet diameter. The normalized Reynolds number is $\mathrm{Re}_p = \frac{\rho\left|\vec{v}_p-\vec{v}\right|d_p}{\mu}$; in the problem under consideration with typical velocities of the air flow in the bronchi, the Reynolds number is $\mathrm{Re}_p < 0.1$. This condition allows the Hadamard-Rybczynski drag law to be used in computations.

The motion of aerosol droplets is an unsteady process. Therefore, unsteady motion of aerosol droplets is considered on the background of a steady gas flow. The time of the steady gas flow and unsteady motion of droplets is 1 s. As the flow rate increases, the velocity of air and, correspondingly, droplets also increases. There are two reasons why the droplets do not reach the alveoli: (1) the droplets stick to the bronchus walls; (2) at a small air flow velocity (small flow rate), the droplets do not have enough time to reach the alveoli. The initial conditions for the droplets are formulated as follows: the velocity at the input of the 0-th bronchus coincides with the gas velocity, and the concentration is consistent with the nebulizer specification (0.3 ml/min). These initial conditions are valid during the entire inspiration time.

The droplet concentration is low; therefore, their influence on the air flow in the bronchi can be neglected. The computation consists of two stages: first, the gas velocity field is calculated, and then, based on this velocity, the droplet trajectories are found. When the droplets fall onto the bronchus walls, they stick to the walls and are eliminated from the further computation.

Some results on precipitation of aerosol droplets in the bronchial tree were reported in [23, 24]. The results of computed precipitation of drug aerosol droplets are presented in Figures 12 and 13. Aerosol droplet precipitation mainly occurs in the region of carinal divergence of the bronchi (Fig. 12).

Fig. 12. Three projections of aerosol droplet precipitation near the carinal bifurcation of bronchi of the 1-st generation. The blue points are the increased images of droplets stuck to the bronchus walls (to make the figure more understandable, we show a representative set of a large number of droplets).

How does the air flow rate affect precipitation of drug aerosol droplets during inspiration? For comparison, we performed simulations for the air flow rates of 20, 25, 40, and 50 l/min

and inspiration time of 1 s (Fig. 13). Reduction of the air flow rate leads to acceleration of droplet precipitation. All droplets settle down before the 16-th bronchus for the flow rate of 20 l/min and before the 22-nd bronchus for the flow rate of 50 l/min. It is seen from the computations that aerosol droplets do not reach alveoli even if inspiration is very deep.

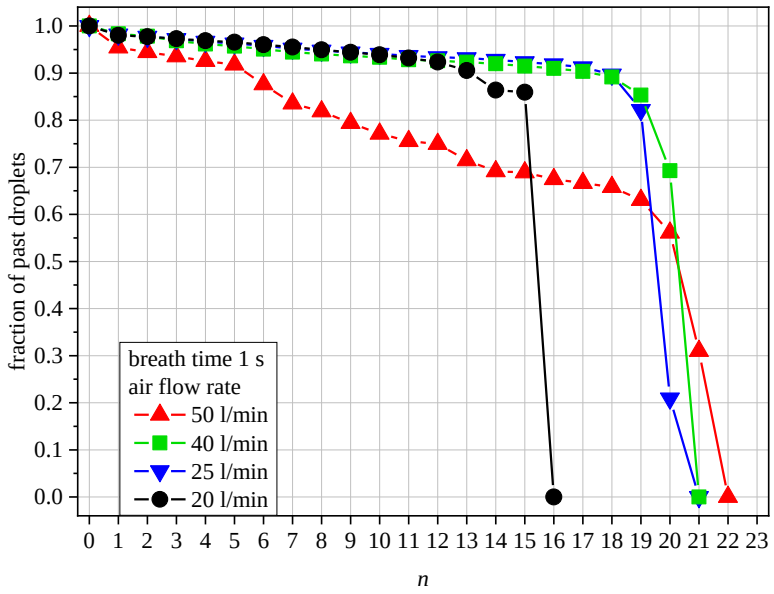

Fig. 13. Fraction of aerosol droplets that passed through the bronchus during 1-s inspiration for the air flow rates of 20, 25, 40, and 50 l/min.

CONCLUSIONS

In our previous publications, we proposed an analytical model for design of the full three-dimensional human bronchial tree [9, 10]. For this model, we developed a method of stage-by-stage numerical simulation of the air flow in human lungs [14]. In the present paper, we tried to demonstrate the possibility of using the method of stage-by-stage computation for typical problems encountered in numerical investigations of air and aerosol flows in human lungs.

The bronchial tree model and the computation method offer the following advantages:

1) simple design of the entire tree (the full bronchial tree is described by analytical formulas);

2) reproducibility of results by other researchers (before now, the results of this or that researcher could not be repeated or checked because it was impossible to reproduce the same bronchial tree geometry);

3) possibility of performing computations in the entire (up to alveoli) bronchial tree (before now, the results were obtained for 17 bifurcations out of 23 at the maximum).

The method of stage-by-stage computation of the bronchial tree ensures accurate numerical simulations in all bronchi because an individual grid is constructed for each bronchus and an individual computation is performed on this grid. The method of stage-by-stage computation of the bronchial tree allows the computation time to be reduced by orders of magnitude. For example, in [12], the time of computing unsteady inspiration up to the 16-th bifurcation takes five days of parallel operation of a computer with the I-7 processor with eight cores, while our simulations take only tens of minutes (for computations up to the 23-rd bifurcation on a computer of a similar class).

The drawback is a simplified model of the bronchial tree (in reality, the bronchial tree has an asymmetric structure and turning of the next bronchus with respect to the previous one by 90º does not always happen). On the other hand, the lung structure for each person has some specific features. The use of this model is justified by the morphometric study of human lungs

and the model of symmetric dichotomy of human lungs proposed in [2], which actually served as a basis for the proposed model of the bronchial tree.

The proposed model of bronchial tree design and the computational method can be applied to a large class of previously considered problems. In the present paper, we demonstrated the possibility of using the method for calculating steady inspiration and steady expiration. In the problem of steady expiration, it was shown that the pressure difference required for steady expiration is greater approximately by 30 % than that in the case of inspiration. It was argued earlier in [13] (erroneously, in our opinion) that the pressure difference is identical in the cases of both inspiration and expiration. It was demonstrated that the numerical results are consistent with the data obtained by other researchers. The results cannot be expected to coincide exactly because the previous computations were performed with a different geometric model of the bronchial tree. Moreover, a laminar air flow model was used in our computations, while the researchers whose results were used here for comparisons used a turbulent model of the air flow in bronchi, which overpredicts the pressure difference.

The model proposed in the paper allows unsteady computations as well. As an example, unsteady inspiration is described.

Using the proposed model, one can compute precipitation of drug aerosol droplets in human lungs. As an example, we computed inspiration of a drug aerosol through a typical compressor nebulizer. Poor efficiency of the nebulizer was demonstrated: even if inspiration is sufficiently deep (50 l/min), the drug droplets do not reach the alveoli (the droplets settle down before the 22-nd bifurcation). Such computations are only possible if the entire human bronchial tree is considered (up to the 23-rd bifurcation). It is impossible to perform such computations by using models of other researchers (where the computations were performed for an incomplete bronchial tree up to the 17-th bifurcation at the maximum).

Thus, the proposed model of bronchial tree design and the method of stage-by-stage computation based on this model offer a possibility of solving a large class of problems necessary for studying the flow of air and aerosols (or particles) in human lungs.

The research was funded by RFBR and Novosibirsk region, project number 20-41-543004.

REFERENCES

1. Peters A., Wichmann H.E., Tuch T., Heinrich J., Heyder J. Respiratory Effects are Associated with the Number of Ultrafine Particles. *Am. J. Respir. Crit. Care Med*. 1997. V. 155. P. 1376–1383. doi: 10.1164/ajrccm.155.4.9105082
2. Weibel E.R. *Morphometry of the Human Lung*. Berlin: Springer Verlag, 1963.
3. Nowak N., Kadake P.P., Annapragada A.V. Computational fluid dynamics simulation of airflow and aerosol deposition in human lungs. *Journal Annals of Biomedical Engineering*. 2003. V. 31. No. 4. P. 374–390. doi: 10.1114/1.1560632
4. Zhang Z., Kleinstreuer C., Kim C.S. Airflow and nanoparticle deposition in a 16-generation tracheobronchial airway model. *Journal Annals of Biomedical Engineering*. 2008. V. 36. No. 12. P. 2095–2110. doi: 10.1007/s10439-008-9583-z
5. Islam M.S., Paul G., Ong H.X., Young P.M., Gu Y.T., Saha S.C. A Review of Respiratory Anatomical Development, Air Flow Characterization and Particle Deposition. *International Journal of Environmental Research and Public Health*. 2020. V. 17. No. 2. P. 380. doi: 10.3390/ijerph17020380
6. Walters D.K., Burgreen G.W., Hester R.L., Thompson D.S., Lavallee D.M., Pruett W.A., Wang X. Cyclic Breathing Simulations in Large-Scale Models of the Lung Airway from the Oronasal Opening to the Terminal Bronchioles. *J. Fluids Eng*. 2014. V. 136. P. 101101. doi: 10.1115/1.4027485

7. Islam M.S., Saha S.C., Sauret E., Gemci T., Yang I.A., Gua Y.T. Ultrafine particle transport and deposition in a large scale 17-generation lung model. *Journal of Biomechanics*. 2017. V. 64. P. 16–25. doi: 10.1016/j.jbiomech.2017.08.028
8. Islam M.S., Saha S.C., Young P.M. Aerosol particle transport and deposition in a CT-based lung airway for helium-oxygen mixture. In: *Proceedings of the 21st Australasian Fluid Mechanics Conference* (*Adelaide, Australia 10–13 Desember 2018*). 2018.
9. Medvedev A.E., Gafurova P.S. Analytical design of the human bronchial tree for healthy patients and patients with obstructive pulmonary diseases. *Mathematical Biology and Bioinformatics*. 2019. V. 14. No. 2. P. 635–648. doi: 10.17537/2019.14.635
10. Medvedev A.E. Method of Constructing an Asymmetric Human Bronchial Tree in Normal and Pathological Cases. *Mathematical Biology and Bioinformatics*. 2020. V. 15. No. 2. P. 148–157. doi: 10.17537/2020.15.t21
11. Tena A.F., Casan P., Fernández J., Ferrera C., Marcos A. Characterization of particle deposition in a lung model using an individual path. *EPJ Web of Conferences*. 2013. V. 45. Article No. 01079. doi: 10.1051/epjconf/20134501079
12. Tena A.F., Francos J.F., Álvarez E., Casan P. A three dimensional in SILICO model for the simulation of inspiratory and expiratory airflow in humans. *Engineering Applications of Computational Fluid Mechanics*. 2015. V. 9. No. 1. P. 187–198. doi: 10.1080/19942060.2015.1004819
13. Tena A.F., Fernández J., Álvarez E., Casan P., Keith Walters D. Design of a numerical model of lung by means of a special boundary condition in the truncated branches. *International Journal for Numerical Methods in Biomedical Engineering*. 2017. V. 33. No. 6. Article No. e2830. doi:10.1002/cnm.2830
14. Medvedev A.E., Fomin V.M., Gafurova P.S. Three-dimensional model of the human bronchial tree – modeling of the air flow in normal and pathological cases. *Journal of Applied Mechanics and Technical Physics*. 2020. V. 61. No. 1. P. 1–13. doi: 10.15372/PMTF20200101
15. Trusov P.V., Zaitseva N.V., Tsinker M.Yu. Modeling of human breath: conceptual and mathematical statements. *Mathematical Biology and Bioinformatics*. 2016. V. 11. No. 1. P. 64–80. doi: 10.17537/2016.11.64
16. Trusov P.V., Zaitseva N.V., Tsinker M.Yu., Babuskina A.V. Modelling dusty air flow in the human respiratory tract. *Russian Journal of Biomechanics*. 2018. V. 22. No. 3. P. 262–274. doi: 10.15593/RZhBiomeh/2018.3.03
17. Miller M.R., Hankinson J., Brusasco V., Burgos F., Casaburi R., Coates A., Crapo R., Enright P., van der Grinten C.P.M., Gustafsson P. et al. Standardisation of spirometry. *European Respiratory Journal*. 2005. V. 26. P. 319–338. doi: 10.1183/09031936.05.00034805
18. Ganimedov V.L., Muchnaya M.I., Sadovskii A.S. Air flow in the human nasal cavity. Results of mathematical modelling. *Russian Journal of Biomechanics*. 2015. V. 19. No. 1. P. 31–44. doi: 10.15593/RZhBiomeh/2015.1.03
19. Fomin V.M., Vetlutsky V.N., Ganimedov V.L., Muchnaya M.I., Shepelenko V.N., Melnikov M.N., Savina A.A. Air flow in the human nasal cavity. *Journal of Applied Mechanics and Technical Physics*. 2010. V. 51. No. 2. P. 233–240. doi: 10.1007/s10808-010-0033-y
20. Ganimedov V.L., Muchnaya M.I. Numerical simulation of particle deposition in the human nasal cavity. *Thermophysics and Aeromechanics*. 2020. V. 27. No. 2. P. 303–312. doi: 10.1134/S0869864320020122
21. Lukyanov G.N., Voronin A.A., Rassadina A.A. Simulation of convective flows in irregular channels on the example of the human nasal cavity and paranasal sinuses. *Technical Physics*. 2017. V. 62. P. 484–489. doi: 10.1134/S1063784217030136
22. Hermes O. *Hadamard-Rybczynski Equation*. Bellum Publ., 2012.

23. Medvedev A.E., Gafurova P.S. Air flow and precipitation of medicine aerosol droplets in the human bronchial tree. *AIP Conference Proceedings*. 2021. V. 2351. No. 1. Article No. 030018. doi: 1063/5.0051724
24. Medvedev A.E., Gafurova P.S. Simulation of the deposition of aerosol droplets in a person's bronchial tree. *Journal of Physics: Conference Series*. 2019. V. 1404. Article No. 012031. doi: 10.1088/1742-6596/1404/1/012031

Received 19.12.2021.
Published 10.01.2022.